

# Photocatalytic Decomposition of Aliphatic Alcohols, Acids, and Esters

M. Catherine Blount, Jason A. Buchholz, and John L. Falconer<sup>1</sup>

Department of Chemical Engineering, University of Colorado, Boulder, Colorado 80309-0424

Received June 26, 2000; revised October 16, 2000; accepted October 17, 2000; published online December 21, 2000

The photocatalytic decomposition (PCD) of aliphatic alcohols, acids, and esters in an inert atmosphere on TiO<sub>2</sub> and Pt/TiO<sub>2</sub> at room temperature was studied using transient reaction techniques. The addition of Pt to TiO<sub>2</sub> increased the rate of reaction and changed the selectivity significantly, even though Pt is not a photocatalyst and does not have a measurable rate of thermal catalytic activity at room temperature. Although none of the reactants decomposed to form H<sub>2</sub> on TiO<sub>2</sub>, significant amounts of H<sub>2</sub> formed for some reactants during on Pt/TiO<sub>2</sub>, presumably because H atoms spill over onto Pt and recombine to form H<sub>2</sub>. Hydrogen formed on Pt/TiO<sub>2</sub> for all the organics with H bonded to the carbon in a –C–O– group. When only alkyl groups were bonded to the carbon in a –C–O– group, alkanes formed but not H<sub>2</sub>. Abstraction of a H atom appears to be the first step in PCD of alcohols, acids, and esters. Alcohols react to form the corresponding aldehyde and either H<sub>2</sub> or alkanes. Acids and esters react similarly through two parallel pathways, and one pathway extracted lattice oxygen. © 2001 Academic Press

## INTRODUCTION

Heterogeneous photocatalytic oxidation (PCO) is a promising technique for the complete oxidation of dilute organic pollutants in waste gas streams. Many organics can be oxidized to CO<sub>2</sub> and H<sub>2</sub>O at room temperature on TiO<sub>2</sub> catalysts in air when illuminated with UV or near-UV light. The UV light excites electrons from the valence band into the conduction band. The resulting electron/hole pairs can then migrate to the surface and initiate redox reactions with adsorbed organics. The rate of PCO can be increased for many organics by adding low concentrations of Pt as small particles supported on the TiO<sub>2</sub> surface (1–6).

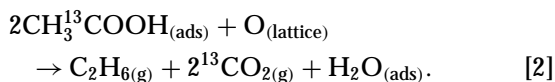
In the absence of gas phase O<sub>2</sub>, photocatalytic reactions also take place on TiO<sub>2</sub> and Pt/TiO<sub>2</sub>, and these reactions are of interest because they may provide insight into the reaction processes that take place during PCO. Moreover, Pt appears to have a large effect on the rate and selectivity for PCD. Thus, the photocatalytic decomposition (PCD) of several aliphatic alcohols, acids, esters, and aldehydes was studied in the absence of O<sub>2</sub> on two Pt/TiO<sub>2</sub> catalysts. The

various organics used helped distinguish which functional groups are most reactive on Pt/TiO<sub>2</sub>.

Photocatalytic decomposition has been studied mainly in the liquid phase on TiO<sub>2</sub> and Pt/TiO<sub>2</sub>, and acetic acid decomposition was used in several studies (7–14). Kraetler and Bard (7) used both acetic acid and sodium acetate solutions, and found that acetic acid decomposed to CH<sub>4</sub> and CO<sub>2</sub> along with small amounts of C<sub>2</sub>H<sub>6</sub> and H<sub>2</sub>. When deuterated acetic acid (CH<sub>3</sub>COOD) was reacted, monodeuterated methane and deuterated hydrogen gas were observed, but C<sub>2</sub>H<sub>6</sub> was not deuterated. They proposed that acetic acid decomposed to CO<sub>2</sub>, CH<sub>3(ads)</sub>, and H<sub>(ads)</sub>. The CH<sub>4</sub> then formed by combination of CH<sub>3(ads)</sub> and H<sub>(ads)</sub> and C<sub>2</sub>H<sub>6</sub> by the combination of two CH<sub>3(ads)</sub>. They suggested that CH<sub>4</sub> may also form by reaction of CH<sub>3(ads)</sub> with H<sub>2O(ads)</sub>. In addition to acetic acid, Kraetler and Bard (7) studied the PCD of propionic, *n*-butyric, *n*-valeric and pivalic acids. They found that these acids decomposed to their corresponding alkane and CO<sub>2</sub>: RCOOH → RH + CO<sub>2</sub>. The dimer product, R–R, was only observed for acetic acid.

Yoneyama *et al.* (8) also observed CO<sub>2</sub>, CH<sub>4</sub>, C<sub>2</sub>H<sub>6</sub>, and H<sub>2</sub> formation during PCD on Pt/TiO<sub>2</sub> of aqueous solutions of acetic acid and sodium acetate. They proposed a mechanism similar to that of Kraetler and Bard (7); however, their mechanism had an additional pathway: CH<sub>3</sub> + CH<sub>3</sub>COOH → CH<sub>4</sub> + ·CH<sub>2</sub>COOH. The authors attributed large amounts of CO<sub>2</sub> to the oxidation of ethanol and acetaldehyde intermediates. Nosaka *et al.* (10, 11) detected methyl radicals during PCD of acetic acid in water using ESR. They suggested that photo-induced holes react with acetic acid to form CO<sub>2</sub>, CH<sub>3</sub>, and H, and that methyl radicals mainly form CH<sub>4</sub> by reacting with H.

Sclafani *et al.* (15) and Muggli and Falconer (16) observed that gas-phase acetic acid decomposes to CH<sub>4</sub>, CO<sub>2</sub>, and small amounts of C<sub>2</sub>H<sub>6</sub> during PCD. Using labeled acetic acid (CH<sub>3</sub><sup>13</sup>COOH), Muggli and Falconer (16) proposed two parallel pathways for acetic acid PCD on TiO<sub>2</sub>:



<sup>1</sup> To whom correspondence should be addressed, Fax: (303)492-4341. E-mail: john.falconer@colorado.edu.



Their results indicated that the first step is dissociation of the O–H bond and PCD then proceeds through the resulting acetate species. They found that lattice oxygen consumed during C<sub>2</sub>H<sub>6</sub> formation was slowly replenished by diffusion from the TiO<sub>2</sub> bulk, or more rapidly by injecting gas-phase O<sub>2</sub>.

Though 2-propanol does not decompose photocatalytically in the absence of O<sub>2</sub> on TiO<sub>2</sub> (17, 18), it decomposes to acetone and H<sub>2</sub> when a low loading of Pt is added to TiO<sub>2</sub> (17–22). Ait-Ichou *et al.* (18) proposed that the initial step in the PCD of gas-phase 2-propanol was the reaction of adsorbed 2-propanol with a photogenerated hole to form the adsorbed alkoxy radical (CH<sub>3</sub>)<sub>2</sub>CHO<sub>(ads)</sub><sup>•</sup>. They investigated the influence of Pt loading on the steady-state PCD activity. The H<sub>2</sub> production rate increased with Pt loading up to 1.5 wt% Pt and was constant at higher loadings for the range studied. They suggested that this behavior was explained by reverse spillover of hydrogen atoms from TiO<sub>2</sub> to the Pt particles where the hydrogen atoms combined to form gas-phase H<sub>2</sub>. For Pt loadings below 1.5%, the migration of the hydrogen to the Pt particles was proposed to be rate determining.

Pichat *et al.* (23, 24) reported that gas-phase ethanol decomposed to acetaldehyde and H<sub>2</sub> during PCD. Only undeuterated hydrogen evolved during PCD of labeled gas-phase ethanol (CD<sub>3</sub>CH<sub>2</sub>OH) (23). The lack of HD or D<sub>2</sub> indicates that the β-hydrogen atoms of simple aliphatic alcohols are not involved in the primary steps of PCD.

The PCO of aliphatic alcohols (22, 25–33) and acids (25, 30, 34, 35) has been studied extensively, but relatively little work has been done on the PCO of esters (25, 36). Aliphatic alcohols and acids oxidize readily during PCO, and no catalyst deactivation was observed during the PCO of various aliphatic alcohols, acids, and methyl formate (25).

In the current study, transient reaction techniques were used to investigate the surface processes involved in PCD and the role of Pt in PCD for gas phase reactants. A monolayer of organic was adsorbed on oxidized Pt/TiO<sub>2</sub>, and excess organic was flushed from the gas phase. The catalyst was then illuminated with near-UV light in the absence of gas-phase O<sub>2</sub>, and reaction products were detected with a mass spectrometer. The role of lattice oxygen was studied by interrupting the PCD and observing how various dark times affected the PCD behavior. Strongly bound species that remained on the surface after PCD were removed and analyzed using temperature-programmed desorption (TPD) and oxidation (TPO). Alcohols, acids, and esters were used. The organics were chosen to provide insight into the reaction pathways and the roles of the acidic and alcoholic oxygen groups. Two Pt loadings on TiO<sub>2</sub> were used for PCD of selected organics to investigate the role of Pt during PCD.

## EXPERIMENTAL METHODS

The apparatus used for PCD, temperature-programmed desorption (TPD), and temperature-programmed oxidation (TPO) was described previously (28). Approximately 30 mg of catalyst was coated as a thin layer on the inside of an annular Pyrex reactor. The catalysts used were Degussa P25 TiO<sub>2</sub> (75% anatase/25% rutile with a BET surface area of 50 m<sup>2</sup>/g), 0.2 wt% Pt/TiO<sub>2</sub>, and 2 wt% Pt/TiO<sub>2</sub>. The platinumized TiO<sub>2</sub> catalysts were prepared by combining Degussa P25 TiO<sub>2</sub> and a H<sub>2</sub>PtCl<sub>6</sub> solution with HCl. Acetic acid and Na<sub>2</sub>CO<sub>3</sub> were added to obtain a pH of 4. Nitrogen was then bubbled through the solution, which was illuminated for 6 h. The catalyst was then washed in distilled H<sub>2</sub>O and dried at 373 K for 24 h. The annular reactor had a 1-mm annular spacing so that high gas flow rates could be maintained to minimize mass transfer effects and rapidly flush gas phase products from the reactor. Twelve near-UV lights (8 W, type F8T5BLB), positioned evenly around the reactor and approximately 2.5 cm from the catalyst film, illuminated the photoreactor. The light intensity at the catalyst surface was measured as 2.5 mW/cm<sup>2</sup>, which is almost an order of magnitude higher than that used by Muggli and Falconer (16, 29–31, 37–39) during transient PCD studies of formic and acetic acid on TiO<sub>2</sub>. The reactor effluent was analyzed with a quadrupole mass spectrometer (Balzers QMA 125). Computer-controlled data acquisition simultaneously monitored and recorded selected mass signals, temperature, and elapsed time. The mass spectrometer signals were calibrated by injecting known quantities of gases or liquids into the appropriate gas stream composition, and the mass signals were corrected for cracking in the mass spectrometer.

Before each experiment, the catalyst was heated to 723 K in a flowing O<sub>2</sub>/He mixture and then cooled to room temperature to create a reproducible surface. Organics were injected upstream of the reactor and allowed to evaporate into the flowing gas and adsorb onto the catalyst. All experiments started with the catalyst saturated with organic. The organics studied were methanol (Aldrich, 99%), ethanol (McCormick Distilling Co.), *t*-butanol (Fisher Scientific, certified), acetaldehyde (Aldrich, 99%), acetone (Fisher Scientific, certified), formic acid (Sigma, 99%), acetic acid (Aldrich, 99.99%), propionic acid (Aldrich, 99.5%), methyl formate (Aldrich, 99%), methyl acetate (Aldrich, 99%), *t*-butyl acetate (Aldrich, 99%), and phenyl acetate (Aldrich, 99%). After exposure to an organic, the reactor was flushed for at least an hour to remove gas-phase organic, so that only reaction of the adsorbed monolayer was studied. Photocatalytic decomposition was studied by illuminating the catalyst in He (100 standard cm<sup>3</sup>/min). The He was purified by flowing through a molecular sieve immersed in liquid N<sub>2</sub>, and the O<sub>2</sub> concentration in the He stream was below the mass spectrometer detection limit. The O<sub>2</sub> concentration during PCD is estimated to be less than 0.3 ppm (16).

The lights were turned on and off periodically for varying lengths of time during PCD to investigate the role of lattice oxygen and surface diffusion on the PCD of the various organics. After PCD, TPD and TPO were performed by heating the catalyst to 723 K and holding at that temperature until all mass signals returned to their original baseline values. Flowing He (100 standard cm<sup>3</sup>/min) was used for TPD, and 20% O<sub>2</sub>/He (100 standard cm<sup>3</sup>/min) was used for TPO.

## RESULTS

### Photocatalytic Decomposition of Alcohols

A monolayer of methanol readily decomposed on 2% Pt/TiO<sub>2</sub> when illuminated with UV light, and the main reaction was dehydrogenation to form H<sub>2</sub> and a surface species, but CO<sub>2</sub> also formed at a low rate. As shown in Fig. 1, H<sub>2</sub> formed almost immediately upon illumination, and its rate was as much as 50 times higher than the rate of CO<sub>2</sub> formation. Although the rate of H<sub>2</sub> formation quickly reached a maximum, the rate of CO<sub>2</sub> increased much more slowly and was still increasing when the lights were turned off after 10 min. The amounts of CO<sub>2</sub> and H<sub>2</sub> that desorbed during PCD are given in Table 1. The TPD spectra following methanol PCD were similar to the TPD spectra of unreacted methanol, and the amounts desorbed are given in Table 2. Methanol PCD on 0.2% Pt/TiO<sub>2</sub> was similar to PCD on 2% Pt/TiO<sub>2</sub>, but the areal H<sub>2</sub> formation rate (normalized by saturation methanol coverage) was about 1.4 times higher on the 2% catalyst. The CO<sub>2</sub> formation rate, however, was higher by a factor of 1.6 on the 0.2% Pt/TiO<sub>2</sub> (Table 3). Methanol did *not* react to a measurable extent during PCD on unplatinated TiO<sub>2</sub>.

The effect of dark time on PCD was studied by turning the UV lights off and then re-illuminating the catalyst after a period of dark time. In Fig. 1 when the catalyst was re-

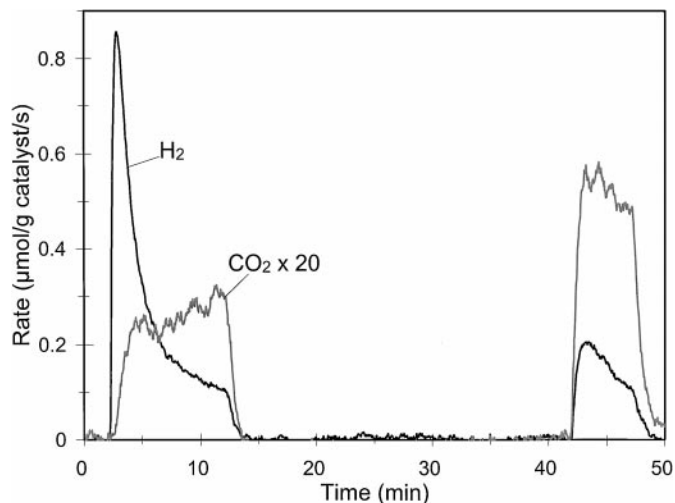


FIG. 1. Photocatalytic decomposition of methanol on 2% Pt/TiO<sub>2</sub>.

TABLE 1  
Desorption Amounts during PCD

| Adsorbed molecule           | Reaction time (min) | Desorption amount (μmol/g catalyst) |                 |                 |                |         |
|-----------------------------|---------------------|-------------------------------------|-----------------|-----------------|----------------|---------|
|                             |                     | H <sub>2</sub>                      | CH <sub>4</sub> | CO <sub>2</sub> | Other organics | Total C |
| 2 wt% Pt/TiO <sub>2</sub>   |                     |                                     |                 |                 |                |         |
| Methanol                    | 15                  | 224                                 |                 | 15              |                | 15      |
| <i>t</i> -butanol           | 15                  |                                     | 173             | 31              | 70             | 337     |
| Formic acid                 | 15                  | 105                                 |                 | 158             |                | 158     |
| Acetic acid                 | 30                  |                                     | 237             | 257             | 13             | 520     |
| Propionic acid              | 40                  |                                     |                 | 335             | 316            | 967     |
| Methyl formate              | 50                  | 313                                 |                 | 206             |                | 206     |
| Methyl acetate              | 15                  | 92                                  | 90              | 92              |                | 182     |
| <i>t</i> -Butyl acetate     | 15                  |                                     | 69              | 68              | 31             | 99      |
| Acetaldehyde                | 10                  |                                     |                 | 17              | 17             | 51      |
| Acetone                     | 15                  |                                     | 22              | 9               |                | 31      |
| 0.2 wt% Pt/TiO <sub>2</sub> |                     |                                     |                 |                 |                |         |
| Methanol                    | 10                  | 106                                 |                 | 21              |                | 21      |
| Ethanol                     | 10                  | 82                                  |                 | Trace           |                | Trace   |
| Formic acid                 | 10                  | 80                                  |                 | 87              |                | 87      |
| Acetic acid                 | 10                  |                                     | 68              | 71              | 4              | 147     |
| Propionic acid              | 15                  |                                     |                 | 231             | 236            | 944     |
| Methyl formate              | 35                  | 243                                 |                 | 100             |                | 100     |

illuminated after 30 min in the dark, the H<sub>2</sub> formation rate doubled, and the CO<sub>2</sub> rate was approximately 1.7 times higher than the rate before the dark time. The CO<sub>2</sub> rate increased with time before the dark time, but it decreased when PCD was restarted after the dark time (Fig. 1).

Ethanol PCD was similar to that for methanol; only gas-phase H<sub>2</sub> and CO<sub>2</sub> formed, and the H<sub>2</sub> rate was 90 times higher than the CO<sub>2</sub> rate. The maximum H<sub>2</sub> formation rate during ethanol PCD was ~0.5 μmol/g catalyst/s. As with methanol, no PCD reaction was detected on unplatinated TiO<sub>2</sub>. During TPD after ethanol PCD on Pt/TiO<sub>2</sub>, unreacted ethanol and its decomposition products,

TABLE 2  
Desorption Amounts during TPD and TPO

| Adsorbed molecule           | Amount desorbed during TPD (μmol/g catalyst) |                 |     |                 |                | TPO (CO <sub>2</sub> ) | Total C |
|-----------------------------|--|-----------------|-----|-----------------|----------------|------------------------|---------|
|                             | H <sub>2</sub>                               | CO <sub>2</sub> | CO  | CH <sub>4</sub> | Other organics |                        |         |
| 2 wt% Pt/TiO <sub>2</sub>   |  |                 |     |                 |                |                        |         |
| Methanol                    | 250  | 94              | 196 | 7               | 36             | 4                      | 337     |
| <i>t</i> -butanol           | 49   | 44              | 63  | 49              | 48             | 98                     | 427     |
| Formic acid                 | 128  | 162             | 109 |                 |                | <1                     | 271     |
| Acetic acid                 | 71   | 97              | 120 | 72              |                | 24                     | 313     |
| Methyl acetate              | 265  | 132             | 292 | 119             | 41             | 28                     | 694     |
| Methyl formate              | 100  | 118             | 93  |                 | 40             | 106                    | 397     |
| <i>t</i> -Butyl acetate     | 82   | 48              | 83  | 6               | 37             | 126                    | 387     |
| 0.2 wt% Pt/TiO <sub>2</sub> |  |                 |     |                 |                |                        |         |
| Methyl formate              | 251  | 152             | 214 |                 | 29             | 11                     | 435     |

TABLE 3

Maximum Areal Rates for 0.2 and 2% Pt/TiO<sub>2</sub>

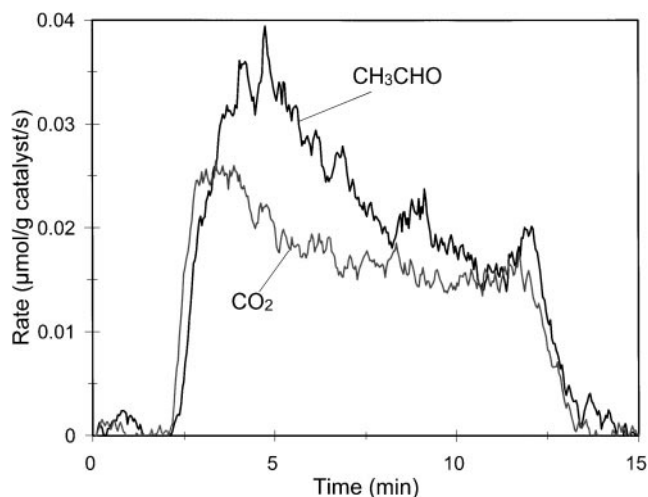
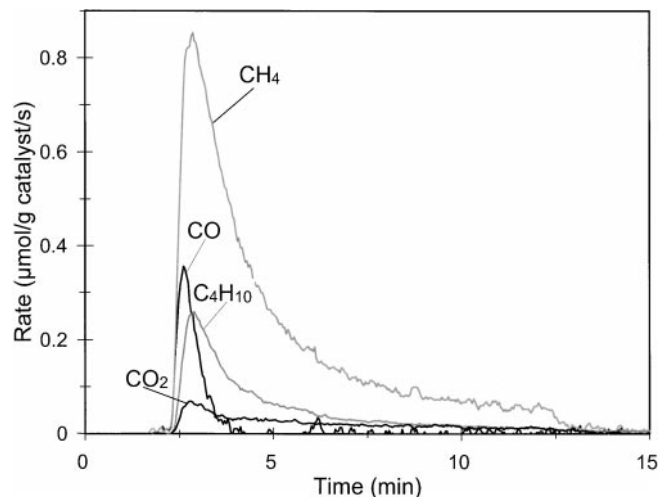
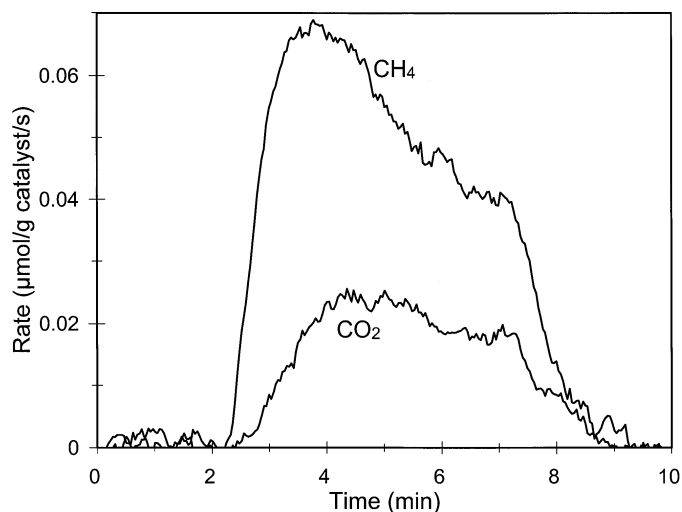
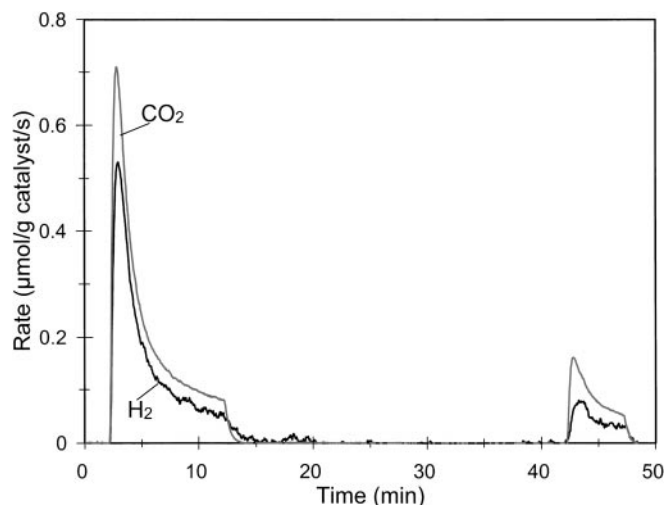
| Adsorbed molecule | Maximum rates $\times 10^4$<br>( $\mu\text{mol/g catalyst/s}$ )/( $\mu\text{mol/g}$ ) |                 |                           |                 |
|-------------------|---|-----------------|---------------------------|-----------------|
|                   | 0.2 wt% Pt/TiO <sub>2</sub>   |                 | 2 wt% Pt/TiO <sub>2</sub> |                 |
|                   | H <sub>2</sub>  | CO <sub>2</sub> | H <sub>2</sub>            | CO <sub>2</sub> |
| Methanol          | 19  | 1.4             | 26                        | 0.89            |
| Formic acid       | 14  | 14              | 13                        | 18              |
| Acetic acid       | —   | 21              | —                         | 39              |
| Methyl formate    | 13  | 5               | 15                        | 9               |

acetaldehyde, ethylene, CO<sub>2</sub>, CO, and H<sub>2</sub>O, desorbed. The PCD of acetaldehyde was performed because acetaldehyde may be a decomposition product during ethanol PCD (23, 24). No H<sub>2</sub> was detected during PCD of a monolayer of acetaldehyde, but as shown in Fig. 2, gas-phase CO<sub>2</sub> and acetaldehyde desorbed.

Photocatalytic decomposition of *t*-butanol was performed because, unlike the primary alcohols, no hydrogens are attached to the alkoxy carbon (–C–OH). During PCD of *t*-butanol, CH<sub>4</sub> was the main product, as shown in Fig. 3, but CO, CO<sub>2</sub>, and butane were also detected. Acetone desorbed during TPD after *t*-butanol PCD, as did unreacted *t*-butanol and its decomposition products. No acetone desorbed during TPD of *t*-butanol when PCD had not been performed prior to TPD. Acetone, like acetaldehyde, was relatively unreactive during PCD on 2% Pt/TiO<sub>2</sub> (Fig. 4); only small amounts of CH<sub>4</sub> and CO<sub>2</sub> formed. The rate of CH<sub>4</sub> formation during acetone PCD was less than 1/10th of the CH<sub>4</sub> formation rate during *t*-butanol PCD.

## Photocatalytic Decomposition of Carboxylic Acids

Formic acid decomposed to form H<sub>2</sub> and CO<sub>2</sub> during PCD on 2% Pt/TiO<sub>2</sub> (Fig. 5). The CO<sub>2</sub> and H<sub>2</sub> peak shapes

FIG. 2. Photocatalytic decomposition of acetaldehyde on 2% Pt/TiO<sub>2</sub>.FIG. 3. Photocatalytic decomposition of *t*-butanol on 2% Pt/TiO<sub>2</sub>.FIG. 4. Photocatalytic decomposition of acetone on 2% Pt/TiO<sub>2</sub>.FIG. 5. Photocatalytic decomposition of formic acid on 2% Pt/TiO<sub>2</sub>.

were similar, but the  $\text{CO}_2$  rate was 1.4 times the  $\text{H}_2$  rate. The remainder of the hydrogen in the formic acid formed  $\text{H}_2\text{O}$ , which was strongly adsorbed on  $\text{TiO}_2$  and desorbed during the subsequent TPD. The TPD after formic acid PCD was characteristic of unreacted formic acid and  $\text{H}_2\text{O}$ , and the carbon and hydrogen mass balance for the PCD and TPD were within 10%. In Fig. 5, after 30 min of PCD, the lights were turned off. When the catalyst was re-illuminated after 30 min in the dark, the  $\text{CO}_2$  and  $\text{H}_2$  formation rates were 1.8 and 1.3 times higher, respectively, than immediately before the dark time. On the 0.2% Pt/ $\text{TiO}_2$ , PCD was similar to that on 2% Pt/ $\text{TiO}_2$ , but the  $\text{CO}_2$  was approximately equal to the  $\text{H}_2$  rate on the 0.2% Pt/ $\text{TiO}_2$  and the maximum formation  $\text{CO}_2$  formation rate was  $\sim 0.45 \mu\text{mol/g catalyst/s}$ .

On  $\text{TiO}_2$  without Pt, only  $\text{CO}_2$  desorbed during formic acid PCD, and no  $\text{H}_2$  formed. The maximum  $\text{CO}_2$  rate on  $\text{TiO}_2$  was only 20% of the rate on 2% Pt/ $\text{TiO}_2$ . Water that formed during PCD was observed during TPD after PCD on  $\text{TiO}_2$ , and the TPD spectra were typical of unreacted formic acid and  $\text{H}_2\text{O}$ .

Gas-phase  $\text{CO}_2$ ,  $\text{CH}_4$ , and ethane formed immediately upon illumination during PCD of acetic acid on 2% Pt/ $\text{TiO}_2$  (Fig. 6), but no  $\text{H}_2$  was observed. After 25 min of PCD and a 30-min dark time, the  $\text{CO}_2$  and  $\text{CH}_4$  formation rates were 4 and 3.3 times higher, respectively, when the catalyst was re-illuminated than immediately before the dark time. On 0.2% Pt/ $\text{TiO}_2$ , the  $\text{CO}_2$  rate was one-third and the  $\text{CH}_4$  rate was one-half of the corresponding rates on 2% Pt/ $\text{TiO}_2$  (Table 3). The  $\text{CO}_2/\text{CH}_4$  ratio was 1.4 for the 2% Pt/ $\text{TiO}_2$ . The remainder of the carbon formed ethane, and the carbon mass balance was within 5% for the PCD on 2% Pt/ $\text{TiO}_2$ . The  $\text{CO}_2/\text{CH}_4$  ratio was roughly 1 for the 0.2% Pt/ $\text{TiO}_2$ , and less ethane formed than on the 2% catalyst. The carbon mass balance on 0.2% Pt/ $\text{TiO}_2$  was within 10%.

Propionic acid ( $\text{CH}_3\text{CH}_2\text{COOH}$ ) reacted through similar pathways to those of acetic acid;  $\text{CO}_2$ , ethane, and bu-

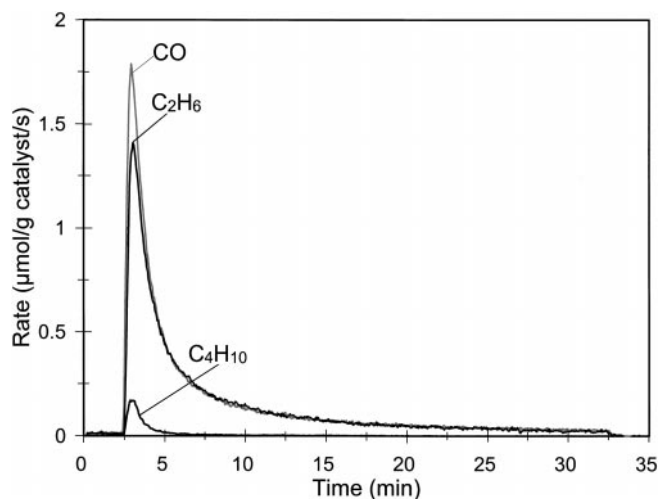


FIG. 7. Photocatalytic decomposition of propionic acid on 2% Pt/ $\text{TiO}_2$ .

tane formed, but no  $\text{H}_2$  formed during PCD on 2% Pt/ $\text{TiO}_2$  (Fig. 7). Though the  $\text{CO}_2$  rate was approximately the same for both 0.2 and 2% Pt/ $\text{TiO}_2$ , the  $\text{C}_2\text{H}_6$  rate was 1.5 times higher on the 0.2% Pt/ $\text{TiO}_2$  catalyst. As with acetic acid, the  $\text{CO}_2/\text{C}_2\text{H}_6$  ratio was 1.4 for the 2% Pt/ $\text{TiO}_2$  and 1 for the 0.2% Pt/ $\text{TiO}_2$ . The remainder of the carbon formed butane, and the carbon mass balance for both catalysts was within 6%.

#### Photocatalytic Decomposition of Esters

During PCD of methyl formate ( $\text{HCOOCH}_3$ ) on 2% Pt/ $\text{TiO}_2$ ,  $\text{H}_2$  and  $\text{CO}_2$  formed immediately upon illumination, as shown in Fig. 8, but no  $\text{CH}_4$  or  $\text{C}_2\text{H}_6$  was observed. The  $\text{H}_2$  rate was approximately 1.7 times the  $\text{CO}_2$  rate. After a 30-min dark time, the  $\text{CO}_2$  and  $\text{H}_2$  formation rates were 3.2 and 3.8 times greater than immediately before the dark

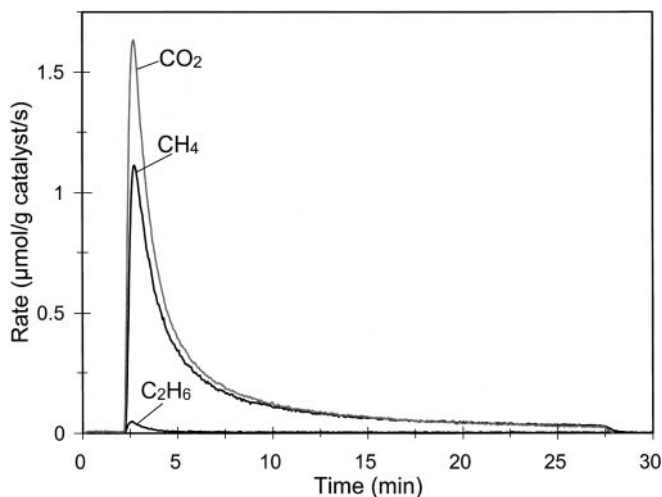


FIG. 6. Photocatalytic decomposition of acetic acid on 2% Pt/ $\text{TiO}_2$ .

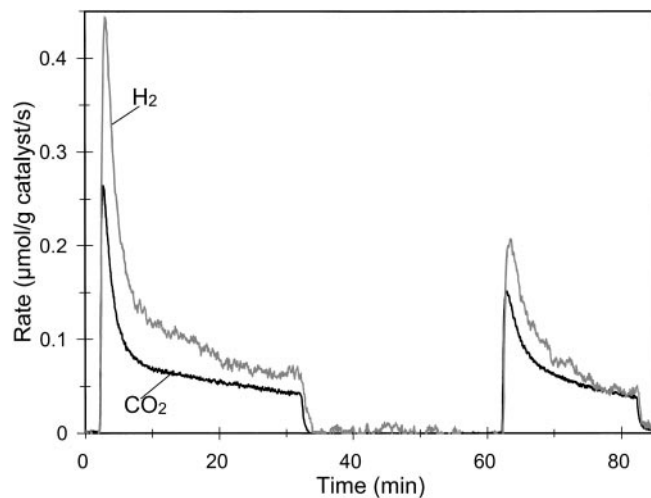


FIG. 8. Photocatalytic decomposition of methyl formate on 2% Pt/ $\text{TiO}_2$ .

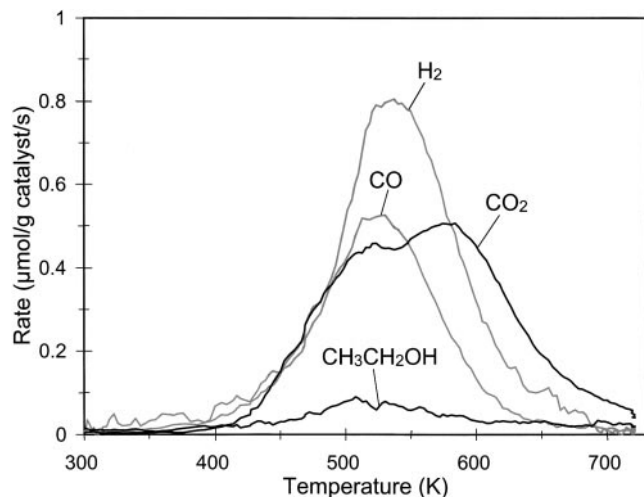


FIG. 9. Temperature-programmed desorption after methyl formate PCD on 2% Pt/TiO<sub>2</sub>.

time, respectively. During TPD after PCD, CO, CO<sub>2</sub>, and H<sub>2</sub> desorbed at high temperatures, and a small amount of ethanol and ethane (not shown for clarity) desorbed (Fig. 9). These spectra, with the exception of the ethane and ethanol formation, are similar to TPD of formic acid (Fig. 10). The desorbing species may also be from the decomposition of unreacted methyl formate or from the decomposition of other unidentified intermediates remaining on the catalyst surface.

During PCD of methyl formate on 0.2% Pt/TiO<sub>2</sub>, the CO<sub>2</sub> formation rate was 55% and the H<sub>2</sub> rate was 85% of the corresponding rates on the 2% Pt/TiO<sub>2</sub> catalyst (Table 3).

Methyl acetate (CH<sub>3</sub>COOCH<sub>3</sub>) decomposed on 2% Pt/TiO<sub>2</sub> to form H<sub>2</sub>, CH<sub>4</sub>, and CO<sub>2</sub> at similar rates (Fig. 11), and a small amount of ethane (not shown) also formed. During the TPD after PCD, unreacted methyl acetate, H<sub>2</sub>, CO,

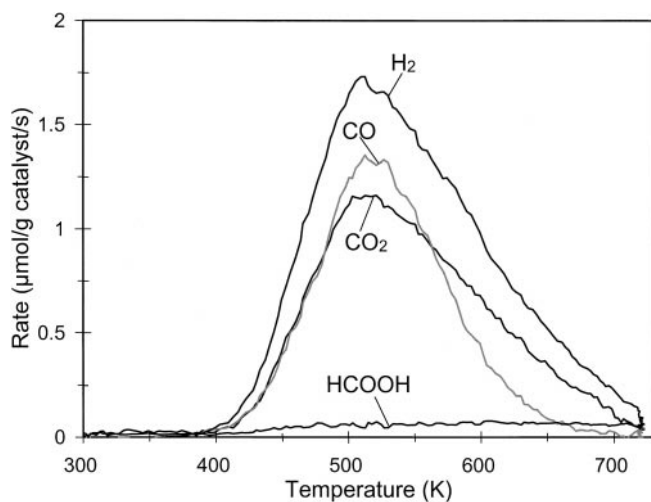


FIG. 10. Temperature-programmed desorption of adsorbed formic acid on 0.2% Pt/TiO<sub>2</sub>.

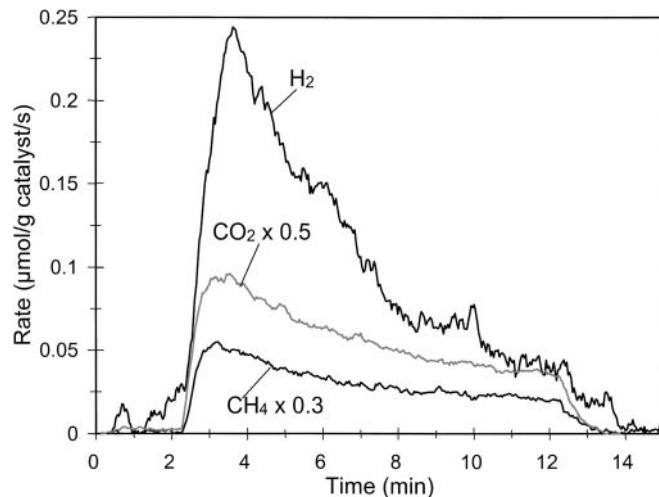


FIG. 11. Photocatalytic decomposition of methyl acetate on 2% Pt/TiO<sub>2</sub>.

CO<sub>2</sub>, and CH<sub>4</sub> desorbed. No measurable reaction occurred during methyl acetate PCD on TiO<sub>2</sub> (16, 35, 37).

Photocatalytic decomposition of *t*-butyl acetate (CH<sub>3</sub>COOC(CH<sub>3</sub>)<sub>3</sub>) formed CH<sub>4</sub>, isobutylene, acetone, and CO<sub>2</sub>, as shown in Fig. 12. The CH<sub>4</sub> and isobutylene rates immediately reached maxima, whereas acetone and CO<sub>2</sub> reached maximum rates after a few minutes of PCD. The CH<sub>4</sub> and isobutylene rates also decreased faster than the acetone and CO<sub>2</sub> rates. After a 30-min dark period, the CH<sub>4</sub> and acetone rates increased only slightly, and no increase was observed for isobutylene and CO<sub>2</sub>.

During TPD after PCD of *t*-butyl acetate (Fig. 13), acetone desorbed in both low and high temperature peaks typical of acetone adsorbed on TiO<sub>2</sub> (28). In addition, isobutylene, CO, CO<sub>2</sub>, H<sub>2</sub>, and CH<sub>4</sub> desorbed. Because CO, CO<sub>2</sub>, H<sub>2</sub>, and CH<sub>4</sub> are all weakly adsorbed on TiO<sub>2</sub>, their

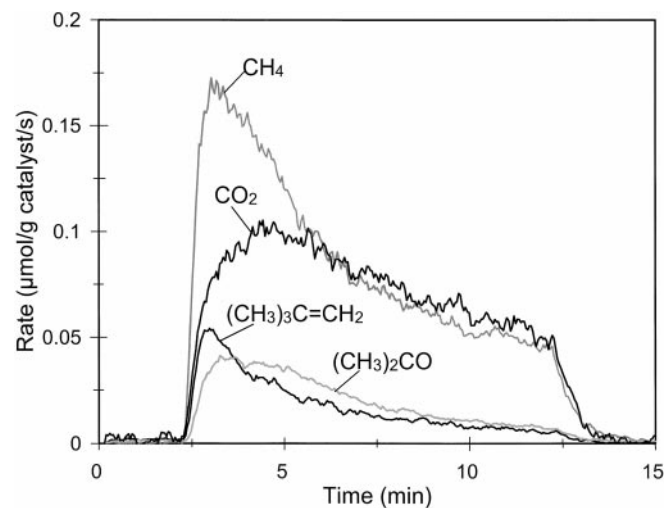


FIG. 12. Photocatalytic decomposition of *t*-butyl acetate on 2% Pt/TiO<sub>2</sub>.

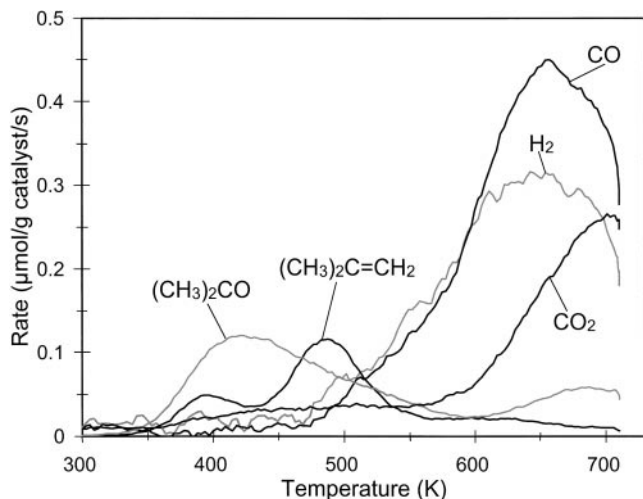


FIG. 13. Temperature-programmed desorption after *t*-butyl acetate PCD on 2% Pt/TiO<sub>2</sub>.

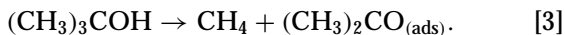
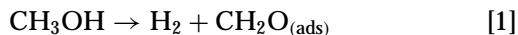
appearance at high temperatures during TPD was due to the decomposition of unreacted *t*-butyl acetate or another intermediate remaining on the catalyst surface. Acetone is strongly adsorbed on TiO<sub>2</sub> (28), so it was probably displaced from the surface during PCD by either water or another intermediate that formed. Isobutylene is not expected to adsorb strongly on TiO<sub>2</sub>. Thus, the isobutylene that desorbed during TPD may be from the decomposition of unreacted *t*-butyl acetate or another intermediate.

Photocatalytic decomposition of phenyl acetate (CH<sub>3</sub>COO-C<sub>6</sub>H<sub>5</sub>) was performed because the hydrogens in the phenyl group are expected to be too strongly bound to participate in reaction. During PCD of phenyl acetate on 2% Pt/TiO<sub>2</sub>, only a trace amount of CO<sub>2</sub> formed, and no other gas-phase species formed.

## DISCUSSION

### Reactions during Photocatalytic Decomposition

The alcohols studied appear to decompose photocatalytically on Pt/TiO<sub>2</sub> to their corresponding aldehydes:



The aldehydes are concluded to form because acetone was detected during TPD following PCD of *t*-butyl alcohol, and acetone was not detected during TPD of adsorbed *t*-butanol when no PCD had been performed. In addition, previous PCD studies of gas- and liquid-phase alcohols on Pt/TiO<sub>2</sub> have observed formation of the corresponding aldehydes (17–19, 23, 24). Pichat *et al.* (23, 24) observed acetaldehyde formation during PCD of liquid ethanol on Pt/TiO<sub>2</sub>.

Moreover, liquid 2-propanol was reported to decompose photocatalytically on Pt/TiO<sub>2</sub> to form H<sub>2</sub>, acetone, and a small amount of CO<sub>2</sub>. Nishimoto *et al.* (17) observed the formation of H<sub>2</sub> and formaldehyde during PCD of aqueous methanol on Pt/TiO<sub>2</sub>. Formaldehyde on TiO<sub>2</sub> decomposes during TPD to form CO and H<sub>2</sub>O (31), and it is expected to decompose faster on Pt/TiO<sub>2</sub>, probably forming CO and H<sub>2</sub>. Thus, formaldehyde was not likely to desorb during TPD after PCD of methanol.

The aldehydes oxidized photocatalytically to form CO<sub>2</sub>, H<sub>2</sub>O, and other products that remain on the surface, but they are much less reactive than the alcohols. Thus much less CO<sub>2</sub> formed than H<sub>2</sub> during methanol and ethanol PCD; indeed, the initial ratios of H<sub>2</sub> to CO<sub>2</sub> were 50 to 90, respectively. The CO<sub>2</sub> rate was higher during acetaldehyde PCD (Fig. 2) than during ethanol PCD because ethanol first decomposes to acetaldehyde. Likewise, approximately 6 times more CH<sub>4</sub> than CO<sub>2</sub> formed during *t*-butanol PCD (Fig. 3), and most of the CH<sub>4</sub> was from *t*-butanol and not acetone decomposition, since only small amounts of CH<sub>4</sub> formed during acetone PCD (Fig. 4). Similarly, all of the H<sub>2</sub> formed during ethanol PCD was from ethanol, since H<sub>2</sub> did not form during acetaldehyde PCD (Fig. 2).

To form CO<sub>2</sub> from the aldehydes, additional oxygen was required, and it was most likely extracted from the TiO<sub>2</sub> lattice to form a reduced surface (16, 35, 39). Indeed, when the Pt/TiO<sub>2</sub> was held in the dark after PCD, the rate of CO<sub>2</sub> formation from methanol PCD was almost twice as high when the lights were turned back on (Fig. 1), as expected if lattice oxygen diffused from the TiO<sub>2</sub> bulk during the dark time (35). The rate of H<sub>2</sub> formation also increased after the dark time even though H<sub>2</sub> formation does not need lattice oxygen; apparently alcohol PCD is faster on oxidized TiO<sub>2</sub>.

In addition to the alcohols decomposing to form aldehydes, which then more slowly oxidized to CO<sub>2</sub>, *t*-butanol had a parallel reaction pathway during PCD to form isobutane and CO. Much less *t*-butanol reacted through this pathway than through reaction [3].

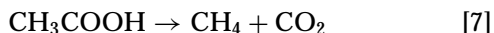
During the first 10 min of methanol PCD on 2% Pt/TiO<sub>2</sub> (Fig. 1), the CO<sub>2</sub> rate increased with time. Since the CO<sub>2</sub> formed from formaldehyde oxidation, the CO<sub>2</sub> rate apparently increased as the formaldehyde concentration increased. In addition, the first CO<sub>2</sub> that formed may have adsorbed on TiO<sub>2</sub>, since a small amount of CO<sub>2</sub> adsorbs on TiO<sub>2</sub>; as the sites for CO<sub>2</sub> adsorption were saturated, CO<sub>2</sub> appeared in the gas phase.

Note that for reactions [1]–[3] and also for PCD of 2-propanol reported in the literature (17–22), H<sub>2</sub> was the primary reaction product if the alcohol possessed a hydrogen bonded to the  $\alpha$ -carbon. Since *t*-butanol does not, it did not form H<sub>2</sub>, but instead split off a CH<sub>3</sub> group, which was hydrogenated. The general reactions are





The same trend was observed for the organic acids; H<sub>2</sub> only formed if H atoms were bonded to the  $\alpha$ -carbon, and otherwise alkanes formed



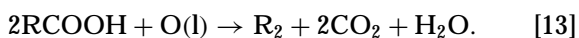
Thus, the general reaction for the acids is



In addition, the acids all exhibited a parallel pathway through which a small fraction of the acid reacted. This pathway was the same as that reported previously for PCD of formic and acetic acid on TiO<sub>2</sub> in which lattice oxygen is extracted to form H<sub>2</sub>O (16, 35, 37):



On Pt/TiO<sub>2</sub>, this secondary pathway has the general form:

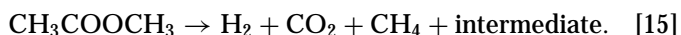


Note that for reactions [9] and [13], the  $\alpha$ -carbon forms CO<sub>2</sub>. Reactions [7], [10], and [11] were also observed for PCD of formic and acetic acid on TiO<sub>2</sub> (16, 35, 37), but H<sub>2</sub> was only observed when Pt was on the surface. On TiO<sub>2</sub>, isotope labeling showed that only the  $\alpha$ -carbon formed CO<sub>2</sub> during PCD. The mass balances for acetic acid and propionic acid products on Pt/TiO<sub>2</sub> are also consistent with the  $\alpha$ -carbon forming CO<sub>2</sub> and the R groups forming alkanes.

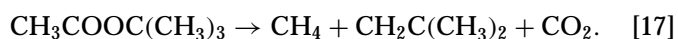
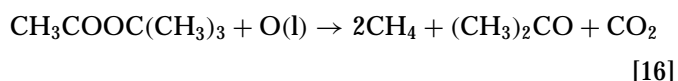
The acetic acid PCD rates reported on TiO<sub>2</sub> by Muggli *et al.* (16, 37) were an order of magnitude lower than those observed in this study on Pt/TiO<sub>2</sub>. Note, however, that the light intensity used in these previous studies was approximately an order of magnitude lower than for this study. After a 10-min PCD of acetic acid on TiO<sub>2</sub> and a 7-min dark period, the CH<sub>4</sub> rate was the same upon re-illumination as it was immediately before the dark period, but the CO<sub>2</sub> and C<sub>2</sub>H<sub>6</sub> rates had increased (16). In our study, all the rates increased after a dark period following acetic acid PCD on 2% Pt/TiO<sub>2</sub>. Additionally, all of the rates increased after a dark period during acetic acid PCD on TiO<sub>2</sub> with the higher light intensity (40). Apparently, reaction [7] was slowed on the reduced surface, even though it does not require lattice oxygen. Because the rates were significantly higher and the reaction time was longer on the Pt/TiO<sub>2</sub> catalyst in the current study than on TiO<sub>2</sub> in the previous studies, more lattice

oxygen was consumed during PCD on Pt/TiO<sub>2</sub>, and thus the effect of the reduced surface on reaction [9] was visible.

The esters followed similar reaction pathways during PCD on Pt/TiO<sub>2</sub>:

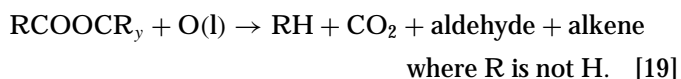
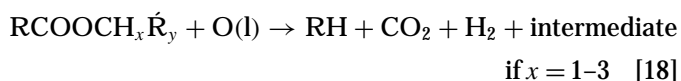


Some adsorbed intermediate, perhaps an aldehyde such as formaldehyde, also formed during methyl acetate and methyl formate PCD. Two reaction pathways were observed for *t*-butyl acetate:

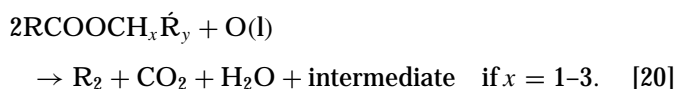


Reaction [16] requires additional hydrogen from either hydrogen radicals or water to balance the chemical equation. As observed for the alcohols and acids, H<sub>2</sub> only formed from esters during PCD when H atoms were bonded to one of the  $\alpha$ -carbons. For methyl formate, the H bound to the acid carbon and H in the methyl group both formed H<sub>2</sub>, so H<sub>2</sub> formed at a higher rate during PCD of methyl formate than methyl acetate. The maximum areal rate for H<sub>2</sub> formation during methyl formate PCD was 1.2 and 1.6 times, respectively, the maximum H<sub>2</sub> rate for formic acid and methyl acetate PCD on 2% Pt/TiO<sub>2</sub>.

The general reaction for esters is

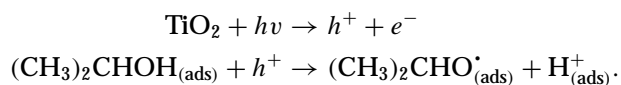


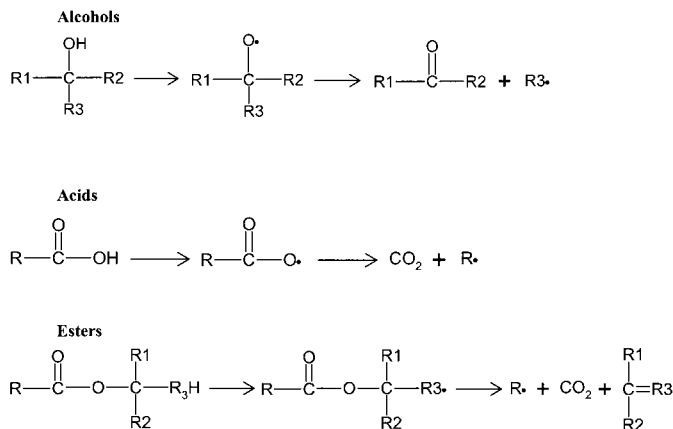
In addition, the esters appear to react through a parallel pathway similar to that observed for acids, but only a small fraction of the ester reacted through this pathway:



### Reaction Mechanisms

Ait-Itchou *et al.* (18) and Pichat *et al.* (24) in their studies of gas-phase isopropanol PCD on Pt/TiO<sub>2</sub> proposed that the reaction is initiated by the reaction of a generated hole with an adsorbed isopropanol molecule:

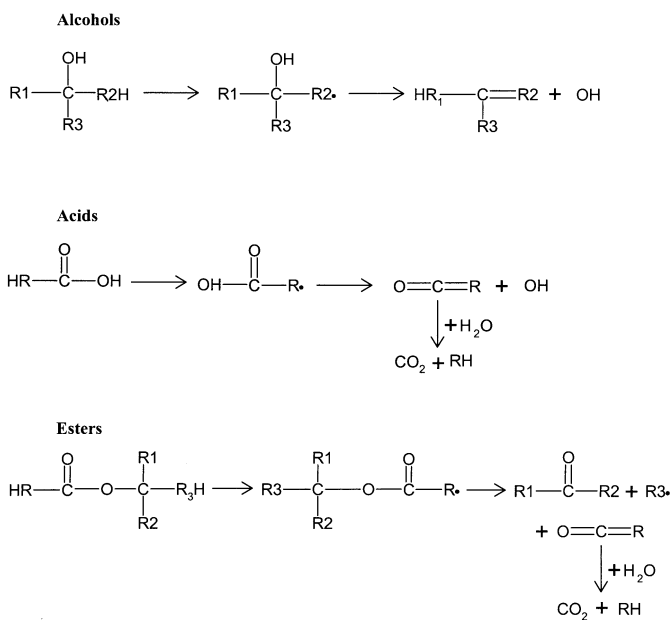




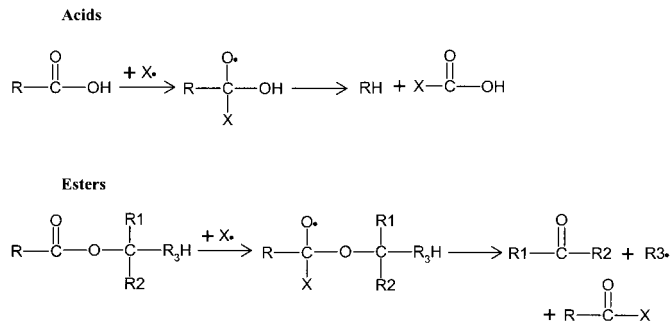
SCHEME 1

In their mechanisms, the  $\text{H}^+$  combine on electron-rich Pt particles to form  $\text{H}_2$ , and  $(\text{CH}_3)_2\text{CHO}\cdot$  reacts to acetone and  $\text{H}_2$ . The decomposition products observed during PCD are consistent with initiation by abstraction of a H (Schemes 1 and 2) or the addition of a nucleophile to the organic molecule (Scheme 3). Although the catalyst was heated to 730 K in an  $\text{O}_2/\text{He}$  flow before each experiment, the  $\text{TiO}_2$  could still be partially covered with hydroxyl groups (41, 42). Hydrogen abstraction could occur from reaction with a hydroxyl radical, direct reaction with an electron or hole, or reaction with some other nucleophile. Several pathways are possible depending on which H is abstracted.

Phenyl acetate was unreactive during PCD on Pt/ $\text{TiO}_2$ . Since the hydrogens on the phenyl group are strongly bound (43), these hydrogens are unavailable for abstraction. Thus, phenyl acetate does not decompose through Scheme 1 for



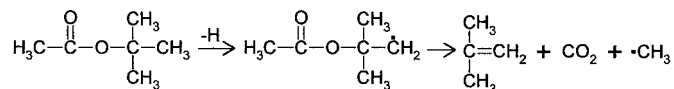
SCHEME 2



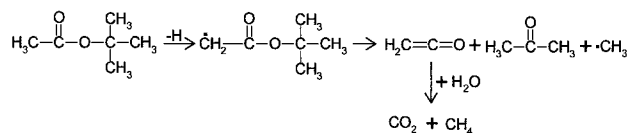
SCHEME 3

esters. Because phenyl acetate was unreactive, this suggests that a H attached to  $-\text{C}-\text{O}-$  or a H attached to  $-\text{R}-\text{C}-\text{O}-$ , where R is an alkyl group, is necessary for PCD to occur, and Schemes 2 and 3 are not significant pathways. In addition, because an alkene did not form during PCD of ethanol or *t*-butanol, abstraction of a H from the R groups attached to the  $\alpha$ -carbon does not appear to be a significant pathway (Scheme 2).

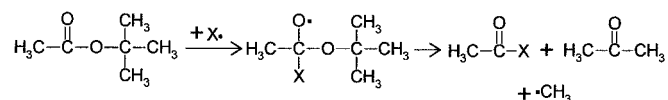
For *t*-butyl acetate, however, Scheme 1 does not fully explain all the reaction products observed. By Scheme 1, *t*-butyl acetate would react to isobutylene,  $\text{CO}_2$ , and  $\text{CH}_3$ , which could then scavenge a H to form  $\text{CH}_4$ :



In addition to these products, acetone also formed during *t*-butyl acetate PCD. Both Schemes 2 and 3 explain acetone formation. Acetone would form by Scheme 2:



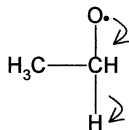
And Scheme 3 would form acetone by



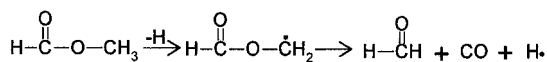
Thus, though PCD initiation may require H attached to  $-\text{R}-\text{C}-\text{O}-$ , where R is an alkyl group, Schemes 2 and/or 3 appear to also play a role during PCD for *t*-butyl acetate.

Because the C-H bond is weaker than the C-C bond,  $\text{H}_2$  forms when H is bound to the  $\alpha$ -carbon, and alkanes are not formed. However, when no H is attached to the  $\alpha$ -carbon, as is the case for *t*-butanol, acetic and propionic acids, methyl acetate, and *t*-butyl acetate, the only decomposition pathway available is alkane formation. For example,

during ethanol PCD, H<sub>2</sub> forms but no methane is observed because the C–H bond is easier to break than the C–C bond:



By Scheme 1, methyl formate is expected to decompose to formaldehyde, H, and CO:

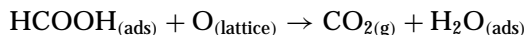


As with the other aldehydes, formaldehyde is expected to react slowly during PCD to CO<sub>2</sub> and H<sub>2</sub>O. No CO was detected during methyl formate PCD; however, any CO that forms may extract lattice oxygen and oxidize to CO<sub>2</sub>, which was detected during PCD.

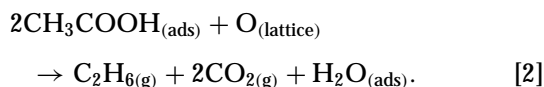
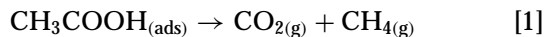
### Effect of Platinum

Platinum has a dramatic effect on the rate of PCD. For example, methanol and ethanol show almost no reactivity on TiO<sub>2</sub> in UV light in the absence of O<sub>2</sub>. On Pt/TiO<sub>2</sub>, however, H<sub>2</sub> formed at high rates as the alcohols dehydrogenated to the corresponding aldehydes. The rate is higher apparently because H atoms spill over from the TiO<sub>2</sub> surface and combine on the Pt surface and H<sub>2</sub> desorbs. On TiO<sub>2</sub>, the rate of H atom recombination is low; since TiO<sub>2</sub> is not a good H<sub>2</sub> dissociation catalyst, it is not effective at recombining H atoms.

Muggli and Falconer (35) reported that formic acid decomposed on TiO<sub>2</sub> to form CO<sub>2</sub> and H<sub>2</sub>O during PCD through the overall reaction:



With the addition of Pt, a significant amount of H<sub>2</sub> formed during PCD, and the areal CO<sub>2</sub> formation rate increased by a factor of 4 (Fig. 5). Muggli and Falconer (16) proposed two parallel pathways for acetic acid PCD on TiO<sub>2</sub>:



They proposed that dissociation of the O–H bond was the first step in PCD. Hydrogen abstraction also appears to be the first step during PCD on Pt/TiO<sub>2</sub>.

Ait-Ichou *et al.* (18) found that larger loadings of Pt dispersed on the TiO<sub>2</sub> surface increased the PCD rate of 2-propanol until a maximum was reached. Past this loading of 1.5 wt% Pt, the H<sub>2</sub> formation rate decreased with increased Pt loading. They proposed that the behavior could

be explained by spillover of hydrogen atoms from the TiO<sub>2</sub> surface onto the Pt particles where the hydrogen combined to form H<sub>2</sub> (44). When the Pt loading was below 1.5%, migration of hydrogen to the Pt particles was rate determining.

Table 3 compares the areal formation rates on 0.2 and 2% Pt/TiO<sub>2</sub> for methanol, formic acid, acetic acid, and methyl formate. During methanol PCD, the maximum areal H<sub>2</sub> rate on 2% Pt/TiO<sub>2</sub> was almost 1.5 times that on 0.2% Pt/TiO<sub>2</sub>, but the maximum CO<sub>2</sub> areal rate was only 60% of that on the 0.2% Pt/TiO<sub>2</sub>. Increasing the Pt loading increased methanol dehydrogenation to formaldehyde by providing more sites for H atom combination. The formaldehyde oxidation rate decreased, however, with Pt loading, perhaps because Pt blocks lattice oxygen sites. Linsbiger *et al.* (45) observed that Pt, when deposited on TiO<sub>2</sub>, titrated oxygen vacancy sites and thus the CO oxidation rates were lower at low temperature. The oxygen vacancy sites were regenerated at high temperatures as the Pt clustered. With more Pt on the surface, more of the sites responsible for aldehyde oxidation may be covered, thus lowering the oxidation rate.

For formic acid PCD, an increase in the Pt loading increased the areal CO<sub>2</sub> rate but had essentially no effect on the H<sub>2</sub> rate. The CO<sub>2</sub> and H<sub>2</sub> signals are similar during formic acid PCD, and the only other species presumably formed is H<sub>2</sub>O. Thus, the overall rate of formic acid decomposition increased with the higher Pt loading, and apparently the rate of H<sub>2</sub>O formation also increased. For methyl formate, the higher Pt loading increased the CO<sub>2</sub> formation rate by 80%, but only increased the H<sub>2</sub> rate by 20%. As with formic acid, the overall rate of methyl formate increased with the higher loading of Pt, and the overall rate of H<sub>2</sub>O formation is presumed to increase also.

The higher loading of Pt increased the rate of acetic acid decomposition, and the CO<sub>2</sub>/CH<sub>4</sub> ratio also increased. Because the results on both 2 and 0.2% Pt/TiO<sub>2</sub> are consistent with the alkoxy carbon forming CO<sub>2</sub> and the methyl carbon forming CH<sub>4</sub> and ethane, the increase in the CO<sub>2</sub>/CH<sub>4</sub> ratio suggests that the rate of pathway 2 proposed by Muggli and Falconer (16) increased. Thus, more ethane was formed at the expense of CH<sub>4</sub>. A similar effect was observed for propionic acid. Thus, for all acids the PCD rates were higher for higher Pt loadings.

### Effect of Dark Time

Muggli and Falconer (16, 35) concluded that lattice oxygen was consumed during acetic acid and formic acid PCD. They showed that following PCD, oxygen diffused from bulk TiO<sub>2</sub> to the surface in the dark and replenished the lattice oxygen. Thus, the PCD rate was higher after an extended dark time. This same behavior was observed on Pt/TiO<sub>2</sub> for formic and acetic acid PCD, indicating that similar reaction pathways take place on Pt/TiO<sub>2</sub>.

The PCD rates on Pt/TiO<sub>2</sub> also increased after an extended dark time for propionic acid, alcohols, methyl

formate, and methyl acetate. Note that the PCD rate of the alcohols was much lower in the absence of Pt. The mass 32 signal did not change during or after PCD, indicating that an O<sub>2</sub> impurity did not affect the PCD rates. Presumably, the only PCD product from the acids that required additional oxygen was H<sub>2</sub>O, but both CO<sub>2</sub> and H<sub>2</sub>O produced during alcohol PCD required additional oxygen. The formation of H<sub>2</sub>O and CO<sub>2</sub> consumed lattice oxygen and reduced the TiO<sub>2</sub>. During the dark time, lattice oxygen was replenished, and the surface was reoxidized so that the rates were higher when the lights were turned back on. The PCD rate after the dark period was not as high as the initial PCD rate because less organic was on the surface and because the dark time was not long enough for the complete oxidation of the catalyst surface. The PCD rates of pathways that did not consume lattice oxygen also increased following a dark time, apparently because the PCD rates were higher on oxidized TiO<sub>2</sub> than on reduced TiO<sub>2</sub>. During PCD of *t*-butyl acetate, only the CH<sub>4</sub> and acetone rates increased after a 30-min dark period, and the CO<sub>2</sub> and isobutylene rates were the same as immediately before the dark time. In the mechanism proposed for *t*-butyl acetate PCD, lattice oxygen is only required for the pathway that produces acetone; thus, the isobutylene rate is not expected to increase after a dark period.

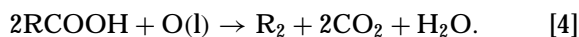
For methyl formate and methanol, the relative ratios of the desorbing products were slightly different immediately before the dark time and when the PCD was restarted. Immediately before the dark time, the H<sub>2</sub>/CO<sub>2</sub> ratio was 1.5 for methyl formate, and the ratio changed to 1.7 after the catalyst was re-illuminated. A similar change was observed for the CO<sub>2</sub>/H<sub>2</sub> ratio during methanol PCD. After 30 min of dark time, the catalyst surface was not completely reoxidized. With this partial surface reduction, the rate of one step of the reaction mechanism, such as dehydrogenation, may increase more than the rate of another step of the reaction mechanism resulting in a change in the product ratios.

## CONCLUSIONS

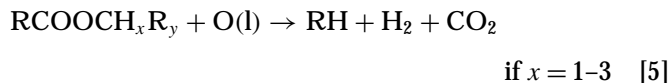
Aliphatic alcohols, acids, and esters photocatalytically decompose on Pt/TiO<sub>2</sub> at room temperature to form CO<sub>2</sub>, H<sub>2</sub>, and/or alkanes. The general PCD reaction for alcohols is



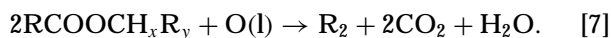
Acids react through two parallel pathways:



Esters also react through two parallel pathways. The first pathway is



and the second pathway is



The PCD pathways are consistent with a reaction mechanism whose first step is hydrogen atom abstraction. Platinum increased the PCD rates dramatically for some reactants, and H<sub>2</sub> formed by spillover of H atoms from TiO<sub>2</sub> to Pt. Hydrogen formed during PCD only when H was bound to an alkoxy carbon. Lattice oxygen was consumed during PCD, and diffusion of bulk oxygen in the dark replenished the lattice oxygen.

## ACKNOWLEDGMENTS

We gratefully acknowledge support by the National Science Foundation, Grant CTS-9714403, and J.A.B. acknowledges support by the NSF-REU Site Grant EEC-9820477. We also thank Professor G. Barney Ellison and Dr. Steve Blanksby of the Chemistry Department at the University of Colorado for valuable discussions.

## REFERENCES

1. Fu, X., Zeltner, W. A., and Anderson, M. A., *Appl. Catal. B* **6**, 209 (1995).
2. Fu, X., Clark, L. A., Zeltner, W. A., and Anderson, M. A., *J. Photochem. Photobiol. A* **97**, 181 (1996).
3. Falconer, J. L., and Magrini-Bair, K., *J. Catal.* **179**, 171 (1998).
4. Izumi, I., Fan, F. R. F., and Bard, A. J., *J. Phys. Chem.* **85**, 218 (1981).
5. St. John, M. R., Furgala, A. J., and Sammells, A. F., *J. Phys. Chem.* **87**, 801 (1983).
6. Takahama, K., Sato, T., Yokoyama, M., and Hirao, S., *Nippon Kagaku Kaishi* **7**, 613 (1994).
7. Kraeutler, B., and Bard, A. J., *J. Am. Chem. Soc.* **100**, 5985 (1978).
8. Yoneyama, H., Takao, Y., and Tamura, H., *J. Phys. Chem.* **87**, 1417 (1983).
9. Sato, S., *J. Phys. Chem.* **87**, 3531 (1983).
10. Nosaka, Y., Koenuma, K., Ushida, K., and Kira, A., *Langmuir* **12**, 736 (1996).
11. Nosaka, Y., Kishimoto, M., and Nishino, J., *J. Phys. Chem. B* **102**, 10279 (1998).
12. Chemseddine, A., and Boehm, H. P., *J. Mol. Catal.* **60**, 295 (1990).
13. Sakata, T., Kawai, T., and Hashimoto, K., *J. Phys. Chem.* **88**, 2344 (1984).
14. Kaise, M., Kondoh, H., Nishihara, C., Nozoye, H., Shindo, H., Nimura, S., and Kikuchi, O., *Chem. Commun.*, 395 (1993).
15. Sclafani, A., Palmisano, L., Schiavello, M., and Augugliaro, V., *New J. Chem.* **12**, 129 (1988).
16. Muggli, D. S., and Falconer, J. L., *J. Catal.* **187**, 230 (1999).
17. Nishimoto, S.-I., Ohtani, B., and Kagiya, T., *Faraday Trans. 1* **81**, 2467 (1985).

18. Ait-Ichou, I., Formenti, M., Pommier, B., and Teichner, S. J., *J. Catal.* **91**, 293 (1985).
19. Ait Ichou, I., Formenti, M., and Teichner, S. J., in "Catalysis on the Energy Scene" (S. Kaliaguine and A. Mahay, Eds.). Elsevier Science, Amsterdam, 1984.
20. Ohtani, B., Iwai, K., Nishimoto, S.-I., and Sato, S., *J. Phys. Chem. B* **101**, 3349 (1997).
21. Scalfani, A., and Herrmann, J.-M., *J. Photochem. Photobiol. A* **113**, 181 (1998).
22. Hussein, F. H., and Rudham, R., *Faraday Trans. 1* **83**, 1631 (1987).
23. Pichat, P., Mozzanega, M.-N., and Courbon, H., *Faraday Trans. 1* **83**, 697 (1987).
24. Pichat, P., Herrmann, J.-M., Disdier, J., Courbon, H., and Mozzanega, M.-N., *New J. Chem.* **5**, 627 (1981).
25. Alberici, R. M., and Jardim, W. F., *Appl. Catal. B* **14**, 55 (1997).
26. Blake, N. R., and Griffin, G. L., *J. Phys. Chem.* **92**, 5697 (1988).
27. Kennedy, J. C. I., and Datye, A. K., *J. Catal.* **179**, 375 (1998).
28. Larson, S. A., Widegren, J. A., and Falconer, J. L., *J. Catal.* **157**, 611 (1995).
29. Muggli, D. S., Larson, S. A., and Falconer, J. L., *J. Phys. Chem.* **100**, 15886 (1996).
30. Muggli, D. S., Lowery, K. H., and Falconer, J. L., *J. Catal.* **180**, 111 (1998).
31. Muggli, D. S., McCue, J. T., and Falconer, J. L., *J. Catal.* **173**, 470 (1998).
32. Nimlos, M. R., Wolfrum, E. J., Brewer, M. L., Fennell, J. A., and Bintner, G., *Environ. Sci. Technol.* **30**, 3102 (1996).
33. Peral, J., and Ollis, D. F., *J. Catal.* **136**, 554 (1992).
34. Kim, D. H., and Anderson, M. A., *Environ. Sci. Technol.* **28**, 479 (1994).
35. Muggli, D. S., and Falconer, J. L., *J. Catal.* **191**, 318 (2000).
36. Chuang, C.-C., Wu, W.-C., Huang, M.-C., Huang, I.-C., and Lin, J.-L., *J. Catal.* **185**, 423 (1999).
37. Muggli, D. S., Keyser, S. A., and Falconer, J. L., *Catal. Lett.* **55**, 129 (1998).
38. Muggli, D. S., and Falconer, J. L., *J. Catal.* **175**, 213 (1998).
39. Muggli, D. S., and Falconer, J. L., *J. Catal.* **181**, 155 (1999).
40. Lee, G. D., Tuan, V. A., and Falconer, J. L., submitted for publication.
41. Wong, J. C. S., Linsebigler, A., Guangquan, L., Fan, J., and Yates, J. T., Jr., *J. Phys. Chem.* **99**, 335 (1995).
42. Lusvardi, V. S., Barteau, M. A., Dolinger, W. R., and Farneth, W. E., *J. Phys. Chem.* **100**, 18183 (1996).
43. Davico, G., Bierbaum, V., Depuy, C., Ellison, G., and Squires, R., *J. Am. Chem. Soc.* **117**, 2590 (1995).
44. Ait-Ichou, I., Formenti, M., and Teichner, S. J., in "Spillover of Adsorbed Species" (G. M. Pajonk, S. J. Teichner, and J. E. Germain, Eds.), p. 63, Elsevier, Amsterdam, 1983.
45. Linsebigler, A., Rusu, C., and Yates, J. T., Jr., *J. Am. Chem. Soc.* **118**, 5284 (1996).